

Similarity of the laser- and thermally annealed Si(111) surfaces

D. M. Zehner and C. W. White

Oak Ridge National Laboratory, Oak Ridge, Tennessee 37830

P. Heimann, B. Reihl, F. J. Himpsel, and D. E. Eastman

IBM T. J. Watson Research Center, Yorktown Heights, New York 10598

(Received 3 August 1981)

Photoemission studies using synchrotron radiation show that laser-annealed Si(111)-(1×1) and Si(111)-(7×7) surfaces have very similar electronic structures; namely, both show (i) the same two surface states (each with a characteristic angular emission pattern), (ii) similar surface core-level spectra, and (iii) the same Fermi-level pinning. We observe that the (1×1) and cleaved (2×1) surfaces are not related as recently reported. Low-energy-electron-diffraction studies conclude that the (1×1) surface has a compressed ideal (1×1) geometry; this is inconsistent with a band-theory interpretation of our results.

It has been recently shown¹⁻³ that atomically clean semiconductor surfaces can be prepared by pulsed-laser-annealing techniques, and, moreover, that such surfaces can be formed with novel atomic arrangements and doping concentrations. The laser-annealed Si(111) surface is of particular interest in that it exhibits an unreconstructed (1×1) diffraction pattern (via low-energy-electron diffraction, LEED); also, a recent dynamical LEED analysis has been made which describes normal incidence LEED data with a model wherein the outer atomic layer is relaxed inwards (compressed) by ~ 0.2 Å and the second layer is expanded by ~ 0.07 Å relative to the ideal (1×1) geometry, with no lateral displacements.³ Theoretical band calculations (for reviews see Ref. 4) predict that such a surface would be metallic, with a half-filled band of dangling bond states at the Fermi energy E_F , and would be very different from the annealed Si(111)-(7×7) and impurity-stabilized Si(111)-(1×1) surfaces as well as from the cleaved Si(111)-(2×1) surface. Recently two studies of laser-annealed Si(111)-(1×1) surfaces have been reported,^{5,6} and it has been suggested⁶ that the laser-annealed (1×1) surface is buckled with no long-range order, but with a short-range (2×1) reconstruction.

We have performed angle-resolved and angle-integrated photoemission studies of both valence-band surface states and surface core-level shifts⁷ for a laser-annealed Si(111)-(1×1) surface prepared in the same manner as was done for the LEED study³ and for a Si(111)-(7×7) surface which was prepared by thermally annealing the (1×1) surface. We find that these two (111) surfaces are remarkably similar; i.e., (1) both show predominant surface states at 0.85 and 1.8 eV below the Fermi level E_F , (2) both show distinctive angular distribution patterns for these two states which are the same, (3) both show the same

Fermi-level position at the surface (within ± 20 meV), and (4) both show similar surface core-level spectra. The principal difference observed between the (1×1) and (7×7) surfaces is that the latter also exhibits a small density of surface states at E_F (metallic surface) which is absent for the (1×1) surface. In contrast with a recent study of a laser-annealed (1×1) surface,⁶ we find that surface-state energies, angular distribution patterns, and surface core-level spectra for the (1×1) and (7×7) surfaces are all quite different from those observed for single-domain and multidomain cleaved Si(111)-(2×1).

These surface states and surface core-level shifts indicate that the laser-annealed (1×1) surface, the impurity-stabilized (1×1) surface,⁸⁻¹⁰ and the Si(111)-(7×7) surface¹¹ all have similar local bonding geometries, and differ only in long-range order which does not drastically alter the local geometry. This conclusion is consistent with the recent LEED studies of Bennett and Webb,¹² who have studied the (7×7) \rightarrow (1×1) phase transition at 1140 K and have found an order-disorder transition. There remains the interesting question of why the LEED analysis³ yields such a good agreement with LEED data using a model (1×1) geometry which appears to be different from that needed to describe the surface electronic structure. One possible explanation is that LEED is not particularly sensitive to the long-range disorder present on the (1×1) surface [compare, e.g., the disordered high-temperature (1×1) phase observed in Ref. 12]. Another explanation is that photoemission can rule out the relaxed ordered (1×1) geometry only if the surface states are band-like as assumed in all calculations to date; i.e., correlation effects not considered to date might be very important for these narrow surface levels.

Experimental photoemission techniques using synchrotron radiation have been described.^{7,13} Surfaces

were prepared from Si(111) wafers (*n*-type 3- Ω cm P-doped) by light sputtering and laser annealing as previously described; an area of ~ 0.7 -cm diameter was annealed with spatially homogeneous ($\pm 20\%$) pulses (typically five pulses) of 2.0 J/cm² using a *Q*-switched pulsed ruby laser. After annealing, these surfaces were characterized using LEED in the preparation chamber, and were then transferred *in situ* to the display spectrometer for photoemission and Auger measurements. Working pressures were $\leq 1 \times 10^{-10}$ Torr.

In Fig. 1, angle-integrated photoemission spectra are presented for a laser-annealed (1 \times 1) surface (full curve) and for a (7 \times 7) surface (dashed curve), which was prepared by annealing the (1 \times 1) surface to ~ 1200 K. For the (1 \times 1) surface, the dashed-dotted line shows the spectrum obtained after a hydrogen exposure [~ 500 L (1 L = 10^{-6} Torr sec) of activated H] which results in about a saturation monolayer coverage of H (same normalization); the difference between the solid curve (a) and the dashed curve within ~ 3 eV of E_F represents surface-state emission. Two predominant surface-state features are seen, (i) at -1.8 eV and (ii) at -0.85 eV, which are essentially identical for both the (1 \times 1) and (7 \times 7) surfaces. For the (7 \times 7) surface, a third weaker feature (iii) is seen at the Fermi level E_F which is at 0.5 ± 0.05 eV above the valence-band maximum E_v (see Ref. 7). These states at E_F , which correspond to $\sim 3\%$ of the total emission intensity from surface states within ~ 3 eV of E_F , appear to originate via the (7 \times 7) reconstruction from the -0.85 -eV states, which show a correspondingly reduced intensity for the (7 \times 7) surface relative to the (1 \times 1) surface.

Angular emission distributions of the (i) -1.8 -eV and (ii) -0.85 -eV surface state for the (1 \times 1) surface are shown in Fig. 2. These were taken with a

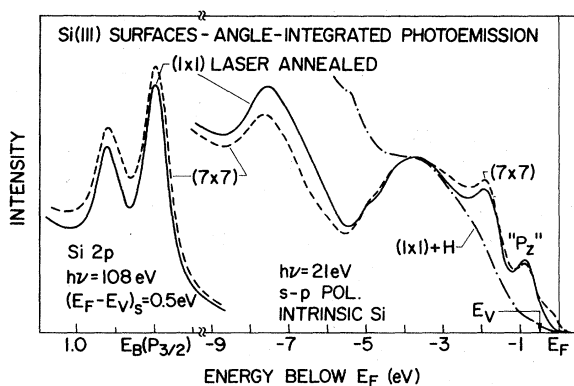


FIG. 1. Angle-integrated photoemission spectra for the valence bands and $2p$ core levels of the laser-annealed Si(111)-(1 \times 1) and thermally annealed Si(111)-(7 \times 7) surfaces. Two prominent surface-state levels are seen for both, i.e., " p_z -like" levels at -0.85 eV and levels at -1.8 eV.

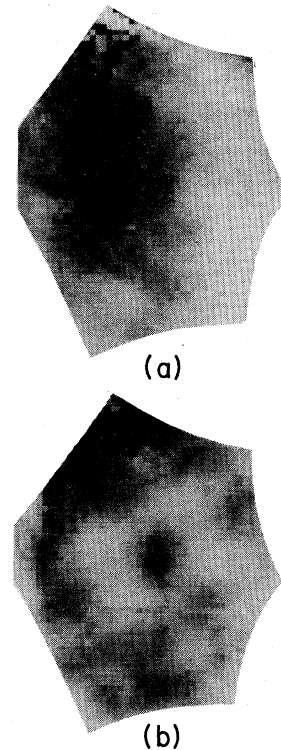


FIG. 2. Pictures showing the angular (momentum) distributions of (a) the -0.85 -eV " p_z -like" surface state and (b) the -1.8 -eV surface state for the Si(111)-(1 \times 1) surface. The hexagonal (1 \times 1) surface Brillouin-zone boundary and zone center as given by our two-dimensional spectrometer system are marked.

display-type photoelectron spectrometer¹³ with mixed *s-p*-polarized radiation (the electric field vector was inclined $\sim 55^\circ$ from the surface normal). The distorted hexagons in Fig. 2 denote the (1 \times 1) hexagonal surface Brillouin zone for the electron energies involved (~ 15 eV) as seen via our display spectrometer. It is seen that surface state (i) at -1.8 eV exhibits a small, sharp emission feature at the zone center $\bar{\Gamma}$, i.e., normal to the surface, and a more intense emission ring near the zone boundary. Surface state (ii) at -0.85 eV exhibits a different pattern, i.e., a broad, diffuse angular emission distribution centered at $\bar{\Gamma}$ with little emission near the zone boundary. The (7 \times 7) surface exhibits essentially identical angular distributions for the corresponding states (not shown). The weak surface-state feature (iii) at E_F which is seen only for the metallic (7 \times 7) surface exhibits a well-defined hexagonal angular emission distribution that is peaked at the Brillouin-zone boundary of a (2 \times 2) surface unit cell (not shown).

Si $2p_{3/2}$ core-level angle-integrated photoemission spectra for the (1 \times 1) and (7 \times 7) surfaces are shown in Fig. 3 (solid lines) for a photon energy $h\nu = 120$ eV, an energy for which the spectra are sur-

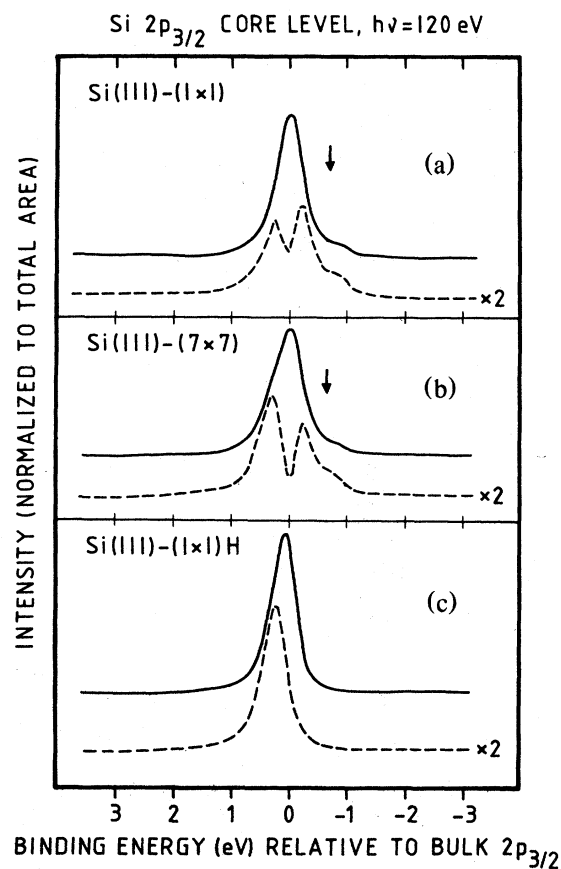


FIG. 3. Si $2p_{3/2}$ core-level spectra for (a) Si(111)-(1 \times 1), (b) Si(111)-(7 \times 7), and (c) Si(111)-H(1 \times 1). The contribution due to the outer double layer of surface atoms is shown by dashed lines.

face sensitive [escape depth $\sim 5.4 \text{ \AA}$ (Ref. 7)] with about $\frac{1}{2}$ the emission intensity corresponding to the outer double layer of Si surface atoms. Following previously described procedures,⁷ we have first decomposed the spectra into similarly shaped $2p_{1/2}$ and $2p_{3/2}$ contributions, and then subtracted from the $2p_{3/2}$ spectra a "bulk" contribution corresponding to the layers below the outer double layer. The resulting curves (dashed lines in Fig. 3) show the spectral distributions of surface core levels for the outer two surface layers (one double layer). In Fig. 3, the energy scale 0 denotes the bulk $2p_{3/2}$ line position. Parameters determined from our fitting (for both surfaces) are a spin-orbit splitting of $\Delta = 0.61 \pm 0.01$ eV, a $2p_{1/2}$ -to- $2p_{3/2}$ branching ratio of 0.51 ± 0.1 at $h\nu = 120$ eV, an electron escape depth of 5.4 \AA for 15-eV photoelectrons, a bulk intrinsic Lorentzian linewidth of $2\Gamma = 0.19$ eV, and an instrumental broadening (Gaussian) of ~ 0.25 eV. The bulk line position, bulk line shape, and instrumental broadening were determined using spectra for hydrogenated surfaces with $h\nu = 108$ eV which have a small surface contribution, as previously described.⁷ The bulk line

positions were found to be the same (within ± 20 meV) for both surfaces; i.e., both have the same band bending at the surface ($E_F - E_v = 0.5 \pm 0.05$ eV). This result disagrees with the band-bending change of -0.15 eV found in Ref. 6 between the (7 \times 7) and (1 \times 1) surfaces. However, the study in Ref. 6 uses valence-band features to determine the band bending which are much broader than the Si $2p$ core levels and affected by surface-state emission.

As seen in Fig. 3, $2p_{3/2}$ surface core-level spectra (dashed curves) for the (1 \times 1) and (7 \times 7) surfaces are very similar, and differ greatly from the spectra for Si(111)-H(1 \times 1). Both show characteristic low-binding-energy peaks, with the (1 \times 1) surface showing a peak at -0.8 eV relative to the bulk with an intensity corresponding to $\sim (\frac{1}{4} \pm \frac{1}{12})$ of a surface layer of atoms and the (7 \times 7) surface showing a peak at -0.7 eV with an intensity corresponding to $\sim (\frac{1}{6} \pm \frac{1}{12})$ of a surface layer of atoms. Both surface spectra also show core levels on the high-binding-energy side of the bulk line at about the same position.

In summary, we have studied valence-band surface states, including both their energy and angular distributions, as well as surface core levels for the laser-annealed (1 \times 1) surface and thermally annealed (7 \times 7) surface and find them to be remarkably similar. This strong similarity indicates that these surfaces have very similar local bonding geometries and differ mainly in long-range order involving geometrical rearrangements that are only a perturbation on the average local bonding geometry. We have also studied cleaved single-domain and multidomain Si(111)-(2 \times 1) surfaces,⁷ and find surface states with different energies ($E_F - 0.5$ eV, $E_F - 1.0$ eV), with different angular distributions, with different surface core-level spectra, and with a different band bending [$E_F - E_v = 0.33$ eV vs 0.51 eV for the (1 \times 1) and (7 \times 7) surfaces]. Thus, we conclude that there are significant differences in the local bonding geometry of the (2 \times 1) vs the (1 \times 1) and (7 \times 7) surfaces. It should be noted that the recently reported study⁶ of laser-annealed Si(111)-(1 \times 1) employed somewhat different experimental conditions [i.e., a Q-switched frequency-doubled Nd-YAG (neodymium-doped yttrium aluminum garnet) laser with a low power such that a multiple-shot raster technique was used to anneal the surface area probed with photoemission and LEED]. Thus somewhat different absorption depths, anneal temperatures, and an about 50% faster regrowth velocity¹⁵ were used, which could result in a different (1 \times 1) surface than the one we have prepared. We do not believe that this causes a different (1 \times 1) surface. Indeed, the surface-sensitive EDC (energy distribution curve) ($h\nu = 21.2$ eV) for Si(111)-(1 \times 1) reported in Ref. 6 has surface states at the same positions as our surface for $h\nu = 21$ eV (Fig. 1) (intensities cannot be compared because of different geometries). In particular, the strong

-1.8-eV surface state exists on the (7×7) and (1×1) surfaces (in our work as well as in Ref. 6) but not on the (2×1) surface.^{7,14}

The question whether a buckling reconstruction takes place on the laser-annealed Si(111) surface (as suggested in Ref. 6) cannot be answered since the geometry of neither the (7×7) nor the (2×1) surface is definitively established at present. We note, in particular, that band calculations for buckled (2×1) surface geometries disagree with recent pho-

toemission data (see Ref. 14).

We wish to acknowledge the support of the University of Wisconsin Synchrotron Radiation Center. Two of us (D.Z. and C.W.W.) were supported in part by the U.S. Air Force Office of Scientific Research (U.S. AFOSR) under Contract No. F49620-80-C-0025. Four of us (P.H., B.R., F.J.H., and D.E.E.) were sponsored by the Division of Materials Sciences, U.S. DOE, under Contract No. W-7405-eng-26 with Union Carbide Corporation.

¹D. M. Zehner, C. W. White, and G. W. Ownby, *Appl. Phys. Lett.* **36**, 56 (1980); **37**, 465 (1980).

²D. M. Zehner, C. W. White, G. W. Ownby, and W. H. Christie, in *Laser and Electron Beam Processing of Materials*, edited by C. W. White and P. S. Peercy (Academic, New York, 1980), p. 201.

³D. M. Zehner, J. R. Noonan, H. L. Davis, and C. W. White, *J. Vac. Sci. Technol.* **18**, 852 (1981).

⁴D. E. Eastman, *J. Vac. Sci. Technol.* **17**, 492 (1980); D. R. Hamann, *Surf. Sci.* **68**, 167 (1977); W. Mönch, *ibid.* **86**, 672 (1979).

⁵A. McKinley, A. W. Parke, G. J. Hughes, J. Fryar, and R. H. Williams, *J. Phys. D* **13**, L193 (1980).

⁶Y. J. Chabal, J. E. Rowe, and D. A. Zwemer, *Phys. Rev. Lett.* **46**, 600 (1981).

⁷F. J. Himpsel, P. Heimann, T.-C. Chiang, and D. E. Eastman, *Phys. Rev. Lett.* **45**, 1112 (1980).

⁸D. E. Eastman, F. J. Himpsel, and J. F. van der Veen, *Solid State Commun.* **35**, 345 (1980).

⁹H. D. Shih, F. Jona, D. W. Jepsen, and P. M. Marcus, *Phys. Rev. Lett.* **37**, 1622 (1976).

¹⁰D. W. Jepsen, H. D. Shih, F. Jona, and P. M. Marcus, *Phys. Rev. B* **22**, 814 (1980).

¹¹D. E. Eastman, F. J. Himpsel, J. A. Knapp, and K. C. Pandey, in *Physics of Semiconductors, 1978*, edited by B. H. Wilson, *Inst. Phys. Conf. Ser. No. 43* (IOP, London, 1979), p. 1059.

¹²P. A. Bennett and M. B. Webb, *Surf. Sci.* **104**, 74 (1981).

¹³D. E. Eastman, J. J. Donelon, N. C. Hien, and F. J. Himpsel, *Nucl. Instrum. Methods* **172**, 327 (1980).

¹⁴F. J. Himpsel, P. Heimann, and D. E. Eastman, *Phys. Rev. B* **24**, 2003 (1981).

¹⁵C. W. White *et al.*, *J. Appl. Phys.* **51**, 738 (1980); D. H. Auston *et al.*, *Appl. Phys. Lett.* **34**, 777 (1979); P. Baeri *et al.*, *ibid.* **37**, 912 (1980). We have found no difference in LEED at 80 K where the regrowth velocity is the same as in Ref. 6.

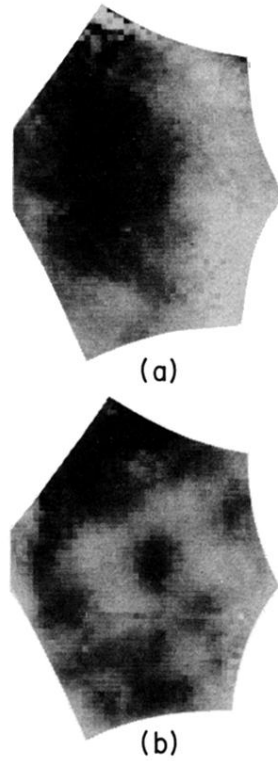


FIG. 2. Pictures showing the angular (momentum) distributions of (a) the -0.85-eV " p_z -like" surface state and (b) the -1.8-eV surface state for the $\text{Si}(111)\text{-}(1 \times 1)$ surface. The hexagonal (1×1) surface Brillouin-zone boundary and zone center as given by our two-dimensional spectrometer system are marked.